Available online at www.sciencedirect.com
ScienceDirect
Bioorganic & Medicinal Chemistry Letters 18 (2008) 2368–2372
Bioorganic & Medicinal Chemistry Letters

TIE-2/VEGF-R2 SAR and in vitro activity of C3-acyl dihydroindazolo[5,4-*a*]pyrrolo[3,4-*c*]carbazole analogs

Ted L. Underiner,* Bruce Ruggeri, Lisa Aimone, Mark Albom, Thelma Angeles, Hong Chang, Robert L. Hudkins, Kathryn Hunter, Kurt Josef, Candy Robinson, Linda Weinberg, Shi Yang and Allison Zulli

Cephalon, Inc., 145 Brandywine Parkway, West Chester, PA 19380-4245, USA

Received 9 January 2008; revised 26 February 2008; accepted 27 February 2008
Available online 4 March 2008

Abstract—Orally bioavailable, dual inhibitors of TIE-2/VEGF-R2 were identified by elaborating the C3/N13 SAR around a fused pyrrolodihydroindazolocarbazole scaffold. Analogs bearing a C3-thiophencarbonyl group were evaluated in enzymatic and cellular biochemical assays; two orally bioavailable analogs were further profiled in functional assays and found to inhibit microvessel growth in rat aortic explant cultures and inhibit Ang-1-stimulated chemotaxis of HUVECs.
© 2008 Elsevier Ltd. All rights reserved.

Angiogenesis, the development of new blood vessels from the endothelium of a pre-existing vasculature, is a critical process required by most solid tumors to support their localized growth and metastatic dissemination within the host. This process entails the proliferation and migration of endothelial cells, the controlled proteolysis of the pericellular matrix, the synthesis of new extracellular matrix components by developing capillaries, the establishment of new intra- and intercellular junctions, and the morphological differentiation of endothelial cells to capillary-like tubular networks providing the rudimentary framework for their subsequent maturation, branching, remodeling and selective regression to a highly organized, functional microvascular network.[1] The pathologic angiogenesis necessary for active tumor growth is sustained and persistent, with the initial acquisition of the angiogenic phenotype being a common mechanism for the development of a variety of solid and hematopoietic tumor types.[1a–d]

Inhibition or neutralization of a single factor or ligand–receptor axis (e.g., VEGF–VEGFR) may not be sufficient for robust inhibition of angiogenesis or tumor growth in every case.[1h,2] Several angiogenic ligands and their corresponding receptor tyrosine kinases that have been implicated in angiogenesis and vasculogenesis, acting at distinct phases spatially and temporally in the angiogenic process in coordinated and complimentary roles to that of the VEGF–VEGFR kinase axes. Principal among these is the angiopoietin family of angiogenic growth factors (Ang-1–4) and their endothelial cell-specific receptor tyrosine kinases, TIE-1 and TIE-2/TEK, which have been implicated in vessel stabilization, maturation and remodeling, and the proper hierarchical organization of the rudimentary vasculature.[1h,2a,3] Further, evidence indicates that inhibition of both TIE-2 and VEGF-R2-mediated signaling results in more dramatic effects on the integrity and stability of both the normal vasculature and the tumor-associated vasculature than inhibition of either pathway alone.[3a,b,4] Thus, optimal anti-angiogenic therapies may necessitate the inhibition of multiple angiogenic targets such as VEGF-R2 and TIE-2. Such a strategy is currently being evaluated clinically[5] and preclinically.[6]

As reported earlier, our second generation pan-VEGF-R dihydroindazolocarbazole (DHI-carbazole) scaffold (2)[7] derived from clinical candidate CEP-7055 (1)[8] possessed inherently potent VEFG-R2 and moderate TIE-2 inhibitory activity (respective IC_{50} values = 16 nM and 1357 nM, Table 1).[9] Engineering the molecular architecture appended to this core provided an effective

Keywords: Kinase inhibitor; VEGF-R2; TIE-2; VEGFR2; Anti-angiogenic.
* Corresponding author. Tel.: +1 610 738 6147; fax: +1 610 344 0065; e-mail: tunderin@cephalon.com

0960-894X/$ - see front matter © 2008 Elsevier Ltd. All rights reserved.
doi:10.1016/j.bmcl.2008.02.069

Table 1. R^3/R^{13} SAR for DHI-carbazoles **5**–**7**

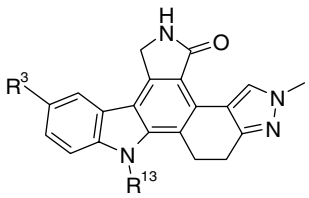

Compound	R^3	R^{13}	TIE-2 IC_{50} (nM)	VEGFR2 IC_{50} (nM)
5a	H	H	1357	16
5b	H	Et	1101	15
5c	H	nPr	136	16
5d	H	*i*-Bu	372	17
6a	Ac	H	>1000[a]	35
6b	Ac	Me	>10K	10
6c	Ac	Et	~1000[b]	13
6d	Ac	Pr	272	3
6e	Ac	Bu	~300[c]	26
6f	Ac	*i*-Pr	726	75
6g	Ac	*i*-Bu	83	21
7a	2-Thiophene-CO	H	136	2
7b	2-Thiophene-CO	Et	43	1
7c	2-Thiophene-CO	Pr	26	5
7d	2-Thiophene-CO	*i*-Pr	24	15
7e	2-Thiophene-CO	*i*-Bu	20	6
8	3-Thiophene-CO	*i*-Bu	63	13
9	2-Furan-CO	*i*-Bu	72	4
10	3-Furan-CO	*i*-Bu	58	8

[a] Inhibition = 28% at 1000 nM.
[b] Inhibition = 50–60% at 1000 nM.
[c] Inhibition = 50–60% at 300 nM.

means to tune the activity against these kinases. The two most amenable sites for synthetic manipulation included the indole N13 and aromatic C3 positions. This paper describes the syntheses and TIE-2/VEGF-R2 SAR, PK and functional activity of C3-acyl substituted DHI-carbazole analogs (**2**, R^3 = COR and R^{13} = alkyl).

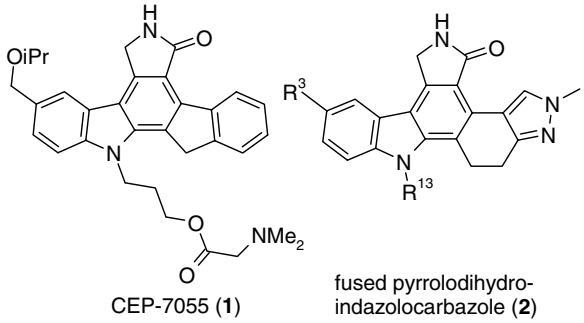

Functionalization of the DHI-carbazole scaffold (**2**) is described in Scheme 1.[9] Although indole alkylation could be carried out on **5**, (R^{13} = H, Cs_2CO_3/MeCN/R^{13}-I), superior yields and easier product isolation were realized if the R^{13} group was installed prior to formation of the fused lactam (e.g., **3**). Friedel–Craft acylation ($AlCl_3$, RCOCl, DCM/$MeNO_2$) proved cleaner with indole-alkylated analogs (i.e., **5**, R13 ≠ H). However, when R^{13} = *i*-Pr (**5e**), $AlCl_3$ induced Friedel–Crafts acylation of **5** occurred concurrently with a substantial degree of indole dealkylation and impeded product isolation. In these instances, $FeCl_3$/DCM/0 °C proved to be a more suitable, synthetic alternative. Such side reactions were not observed with primary (e.g., Et or *i*-Bu) indole substituents.

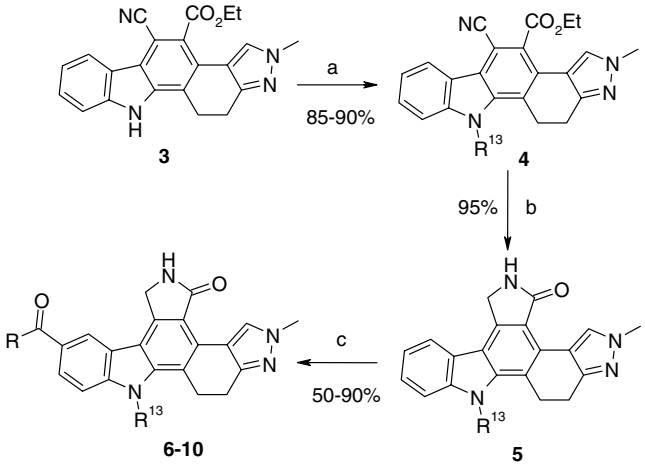

Scheme 1. Tandem alkylation-acylation of DHI-carbazole scaffold. Reagents and conditions: (a) R^{13}-I, acetone, 10 N aq NaOH; (b) RaNi, H_2, DMF/MeOH; (c) RCOCl, $AlCl_3$, DCM/$MeNO_2$ or $FeCl_3$, DCM; yields for Friedel–Crafts acylations were higher with primary- over secondary-R^{13} and with alkyl over aryl acyl chlorides.

The R^3/R^{13} SAR for DHI-carbazole analogs **5**–**7** is summarized in Table 1. For analogs **5** (R^3 = H), VEGF-R2 inhibitory activity was maintained for a variety of R^{13} alkyl substituents; on the other hand, TIE-2 inhibitory activity increased with the length of the R^{13} alkyl chain and Pr and *i*-Bu groups appeared optimal. This trend held when R^3 = Ac (**6**), and 2-thiophenecarbonyl (**7**). Analogs **7b**–**e** demonstrated potent dual inhibition of TIE-2 and VEGF-R2 kinases and had VEGF-R2 cellular IC_{50} values between 10 and 50 nM.[9a,10] In general, analogs with R^{13} = *i*-Bu demonstrated comparable inhibitory activity to those with R^{13} = *n*-Pr, but the former possessed slightly superior solubility properties that facilitated subsequent chemical transformations; therefore the SAR of R^3 was explored with R^{13} as *i*-Bu. Although isomeric 3-thiophenecarbonyl (**8**), 2-furancarbonyl (**9**) and 3-furancarbonyl (**10**) analogs had comparable VEGF-R2 IC_{50} values as 2-thiophenecarbonyl analog (**7e**), their TIE-2 IC_{50} values were typically 3-fold higher. The most potent dual TIE-2/VEGF-R2 inhibitor remained the thiophene DHI-carbazole ketone (**7e**). Therefore the SAR around the thiophene ring was explored especially with regards to optimizing cellular VEGF-R2 inhibition (NIH3T3 cells) and pharmacokinetic properties.

Substitution (methyl or halogens) around the periphery of the thiophene ring of **7e** led to analogs (**7e**–**7i**) that maintained potent VEGF-R2/TIE-2 kinase inhibition; however, TIE-2 inhibition fell 8-fold from **7h** (3-Me) → **7i** (4-Me, Table 2). Cellular inhibition of VEGF-R2 benefited from such modifications with analogs **7g** and **7h** having estimated cellular IC_{50} values

Table 2. Thiophene SAR for analogs of DHI-carbazoles (**7**)

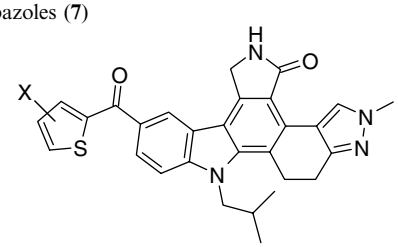

Compound	X	TIE-2 IC_{50} (nM)	VEGFR2 IC_{50} (nM)	VEGFR2 Cell IC_{50} (nM)	PK
7e	H	20	6	10–50	+
7f	3-Cl	13	7	10–50	+
7g	3-Br	15	25	<10	–
7h	3-Me	5	10	<10	–
7i	4-Me	43	11	≫50	–

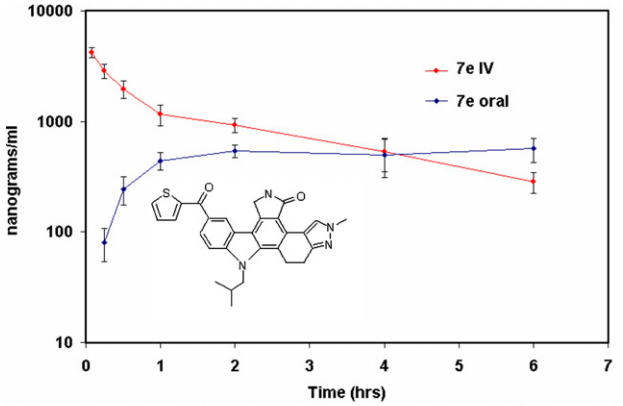

IV 1 mg/kg	7e	Oral 5 mg/kg	7e
$t_{1/2}$, hr	2.32	C_{max}, ng/mL	638
AUC_{0-t}, ng*hr/mL	5679	t_{max}, hr	4
$AUC_{0-\infty}$, ng*hr/mL	6648	AUC_{0-t}, ng*hr/mL	2821
Vd, L/kg	0.52	$AUC_{0-\infty}$, ng*hr/mL	4134
CL, ml/min/kg	2.63	$t_{1/2}$, hr	ND
		estimated oral bioavailability ~ 12%	

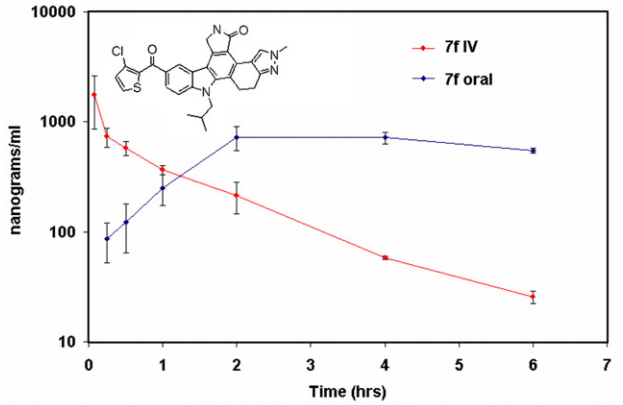

IV 1 mg/kg	7f	Oral 5 mg/kg	7f
$t_{1/2}$, hr	1.35	C_{max}, ng/mL	842
AUC_{0-t}, ng*hr/mL	1443	t_{max}, hr	3.33
$AUC_{0-\infty}$, ng*hr/mL	1492	AUC_{0-t}, ng*hr/mL	3330
V, L/kg	1.4	$AUC_{0-\infty}$, ng*hr/mL	5145
CL, ml/min/kg	12.0	$t_{1/2}$, hr	ND
		Estimated Oral Bioavailability = 69%	

Figure 1. Plasma levels of **7e** and **7f** in rats, 1 mg/kg iv (3% DMSO, 30% solutol), 5 mg/kg po (5:4:1, Tween 80/propylene carbonate/propylene glycol).

<10 nM. However, these latter two analogs had poor intrinsic PK properties (respective Cl values = 138 ± 8 and 72 ± 15 mL/min/kg with AUC values = 123 ± 8 and 261 ± 67 ng h/mL) compared to those for **7e** and **7f** (Fig. 1). In these latter cases, sustained plasma levels >25-fold higher than cellular IC_{50} values (VEGF-R2) could be achieved after oral dosing (5 mg/kg, rat). Despite the low solubility of these analogs (e.g., aqueous solubility at pH = 2.0 and 7.4 for **7e** and **7f** < 1 μg/mL), iv and oral formulations were homogeneous.

To assist in the design of other DHI-carbazole inhibitors and support the SAR, a DFG-in inhibitor binding model of VEGF-R2 described previously was used for docking experiments.[8a] The proposed binding mode for **7e** in this model was consistent with the lactam moiety mimicking the ATP donor–acceptor interactions at the hinge region with the lactam N–H sharing a hydrogen bond with Glu917 carbonyl, and the lactam C=O accepting a hydrogen bond with the backbone amide of Cys919. The C3-thiophenecarbonyl occupied a hydrophobic pocket with the ketone oxygen forming a significant hydrogen bond with Asp1046 and Lys868 as shown in Figure 2.

A similar exercise was carried out to explore putative binding interactions of **7e** with TIE-2.[11] Shown in Figure 3, **7e** was anchored into the hinge region with lactam

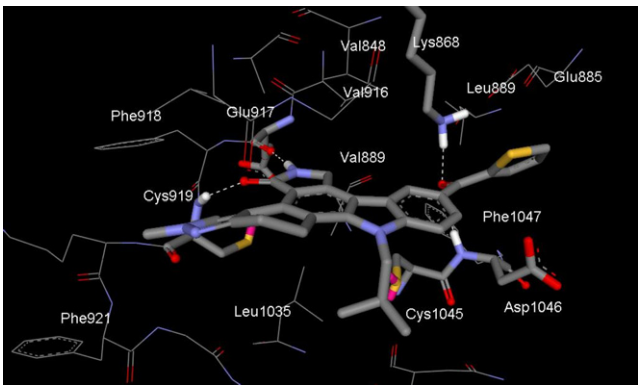

Figure 2. Molecular model depicting **7e** docked into VEGF-R2 ATP pocket.

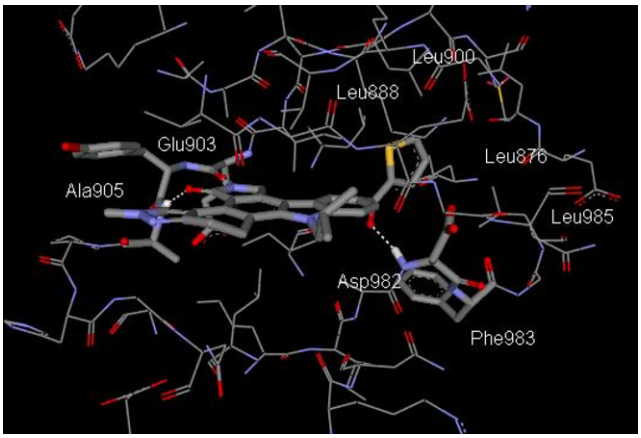

Figure 3. Molecular model depicting **7e** docked into TIE-2 ATP pocket.

N–H and C=O forming a bi-dentate hydrogen bonding interactions with Glu903 carbonyl, and the backbone amide of Ala905. The C3-thienyl ketone occupied a hydrophobic pocket with the carbonyl forming a hydrogen bond with Asp982. The hydrophobic pocket was formed by a series of leucine residues (Leu888, Leu900, Leu876, Leu985), Ala901, Ile902 and Phe983. Figure 3 shows a hydrophobic surface map around **7e**. In this model, the 3-position (see arrow in Fig. 4) appeared more accessible for substitution (**7f**–**h**) than the 4-position (**7i**) which was adjacent to Leu876 (see Figs. 3 and 4), and this may account for the observed SAR favoring **7h** over **7i**.

Two functional assays were used to assess the biological consequences of inhibiting VEGF-R2 and TIE-2. The ex vivo anti-angiogenic activity of thiophene-DHI-carbazole ketones **7e** and **7f** were evaluated in a rat aortic ring explant model, and inhibition of microvessel growth was assessed (Fig. 5).[12] In this model, microvessel growth could be stimulated by a variety of endogenous pro-angiogenic factors including VEGF-R2 and TIE-2. Compounds **7e** and **7f** significantly inhibited the growth of microvessels in a dose dependent manner with estimated EC_{50} values of ~20 nM.

A recombinant human Ang-1-stimulated chemotaxis model was developed to assess inhibition of cell migration of HUVEC cells in a modified Boyden chamber (8 μm pore size) assay. HUVEC cells (10^5 cells/well) and inhibitor (or serum-free media, EBM/0.1% BSA) were seeded into the upper chambers and exposed to Ang-1 (750 ng) in the lower chambers. The cells were allowed to migrate for 16 h through a fibronectin/gelatin-coated filter. After the migration period, the filters were stained with Giemsa solution, the non-migrating cells were removed from the upper side of the filter, and migrated cells were quantified by counting cells in three random fields at 100× magnification per each filter. In contrast to the multiple factors driving rat aortic ring microvessel growth, in this Ang-1-stimulated chemotaxis model, migration was putatively mediated solely by TIE-2, the high-affinity

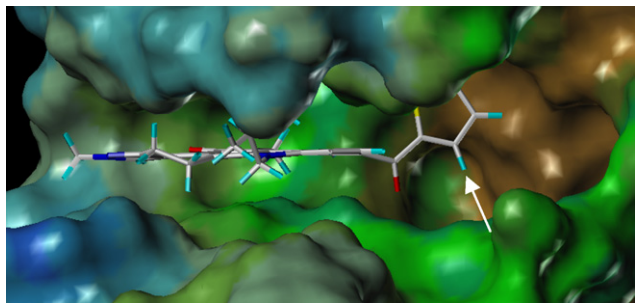

Figure 4. Hydrophobic surface map of TIE-2 ATP pocket around **7e**.

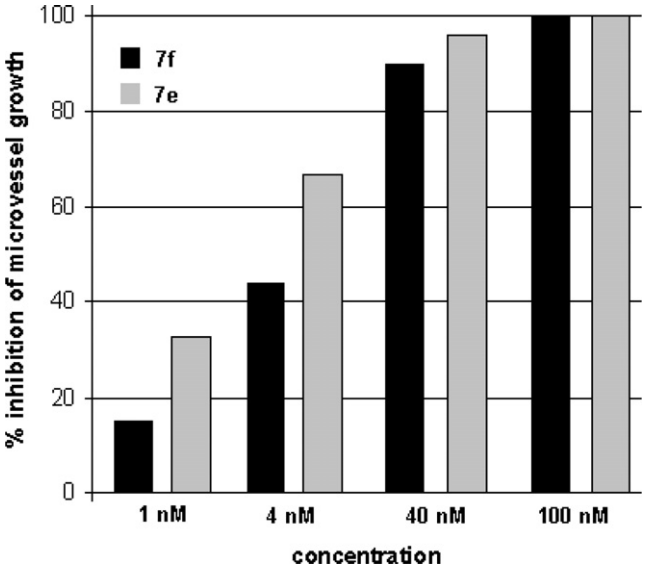

Figure 5. Dose–response (normalized to controls) of **7e** and **7f** for inhibition of microvessel formation from rat aortic ring explants.[11] Microvessels counted in triplicate explant cultures during peak phase (day 8) of microvessel growth ex vivo.

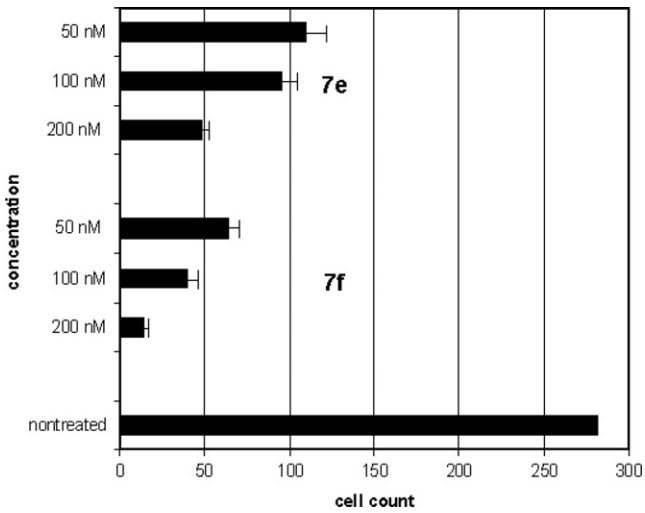

Figure 6. Dose–response of **7e** and **7f** for inhibition of Ang-1-stimulated chemotaxis of HUVECs. Data points represent means + SEM of migrated cell numbers/filter. Assays were done in quadruplicate. Statistical analyses were done by the Student–Newman–Keuls test, with $p < 0.05$ deemed significant.

receptor for Ang-1. Significant dose related inhibition of migration was observed only at concentrations >50 nM (Fig. 6). Furthermore, in both the rat aortic ring assay and the HUVEC chemotaxis assays, no apparent cytotoxicity was evident throughout the course of the experiments (1–7 days).

When screened at 1 μM, analog **7e** demonstrated >80% inhibition of 21 out of a panel of 101 kinases (Millipore).[13] Some of these 21 kinase targets have significant roles in angiogenesis and the regulation of tumor cell growth, progression and survival.

In conclusion, a number of dual inhibitors of TIE-2/VEGF-R2 were identified by elaborating the C3/N13 SAR around a fused pyrrolodihydroindazolocarbazole scaffold that possessed inherently potent VEGF-R2 inhibitory activity. A C-3 carbonyl group conferred potent TIE-2, while maintaining VEGF-R2, inhibitory activity. Two thiophencarbonyl analogs (**7e** and **7f**) were active in functional cellular assays and were orally bioavailable when assessed in rats. The SAR of alternatively C3-substituted DHI-carbazoles is currently being pursued,[7,14] and their in vivo anti-angiogenic and anti-tumor properties in murine models will be reported separately.

References and notes

1. (a) Carmeliet, P.; Jain, R. K. *Nature* **2000**, *407*, 249; (b) Hanahan, D. *Science* **1997**, *277*, 48; (c) Griffioen, A. W.; Molema, G. *Pharmacol. Rev.* **2000**, *52*, 237; (d) Folkman, J. In *Cancer Medicine*, 5th ed.; Holland, J. E., Frei, I. E., Bast, J., Kufe, D., Pollock, R., Weichselbaum, R., Eds.; Dekker, Inc.: Ontario, 2000; pp 132–152; (e) Korpelainen, E. I.; Alitalo, K. *Curr. Opin. Cell Biol.* **1998**, *10*, 159; (f) Ferrara, N.; Davis-Smyth, T. *Endocrine Rev.* **1997**, *18*, 4; (g) Neufeld, G.; Cohen, T.; Gengrinovitch, S.; Poltorak, Z. *FASEB J.* **1999**, *13*, 9; (h) Gale, N. W.; Yancopoulos, G. D. *Gene Dev.* **1999**, *13*, 1055.
2. (a) Jones, N.; Iljin, K.; Dumont, D. J.; Alitalo, K. *Nat. Rev. Mol. Cell Biol.* **2001**, *2*, 257; (b) Giordano, F.J.; (c) Johnson, R. S. *Curr. Opin. Gen. Dev.* **2001**, *11*, 35; (d) Cristofanilli, M.; Charnsangavej, C.; Hortobagyi, G. N. *Nat. Rev. Drug Disc.* **2002**, *1*, 415.
3. (a) Uemura, A.; Ogawa, M.; Hirashima, M.; Fujiwara, T.; Koyama, S.; Takagi, H.; Honda, Y.; Wiegand, S. J.; Yancopoulos, G. D.; Nishikawa, S.-I. *J. Clin. Invest.* **2002**, *110*, 1619; (b) Visconti, R. P.; Richardson, C. D.; Sato, T. N. *Proc. Natl. Acad. Sci. U.S.A.* **2002**, *99*, 8219; (c) Tsigkos, S.; Koutsilieris, M.; Papapetropoulos, A. *Expert Opin. Invest. Drugs* **2003**, *12*, 933.
4. (a) Asahara, T.; Chen, D.; Takahashi, T.; Fujikawa, K.; Kearney, M.; Magner, M.; Yancopoulos, G. D.; Isner, J. M. *Circ. Res.* **1998**, *83*, 233; (b) Lobov, I. B.; Brooks, P. C.; Lang, R. A. *Proc. Natl. Acad. Sci. U.S.A.* **2002**, *99*, 11205.
5. Beebe, J. S.; Jani, J. P.; Knauth, E.; Goodwin, P.; Higdon, C.; Rossi, A. M.; Emerson, E.; Finkelstein, M.; Floyd, E.; Harriman, S.; Atherton, J.; Hillerman, S.; Soderstrom, C.; Kou, K.; Gant, T.; Noe, M. C.; Foster, B.; Rastinejad, F.; Marx, M. A.; Schaeffer, T.; Whalen, P. M.; Roberts, W. G. *Cancer Res.* **2003**, *63*, 7301.
6. (a) Hasegawa, M.; Nishigaki, N.; Washio, Y.; Kano, K.; Harris, P. A.; Sato, H.; Mori, I.; West, R. I.; Shibahara, M.; Toyoda, H.; Wang, L.; Nolte, R. T.; Veal, J. M.; Cheung, M. *J. Med. Chem.* **2007**, *50*, 4453; (b) Ji, Z.; Ahmed, A. A.; Albert, D. H.; Bouska, J. J.; Bousquet, P. F.; Cunha, G. A.; Glaser, K. B.; Guo, J.; Li, J.; Marcotte, P. A.; Moskey, M. D.; Pease, L. J.; Stewart, K. D.; Yates, M.; Davidsen, S. K.; Michaelides, M. R. *Bioorg. Med. Chem. Lett.* **2006**, *16*, 4326; (c) Miyazaki, Y.; Tang, J.; Maeda, Y.; Nakano, M.; Wang, L.; Nolte, R. T.; Sato, H.; Sugai, M.; Okamoto, Y.; Truesdale, A. T.; Hassler, D. F.; Nartey, E. N.; Patrick, D. R.; Ho, M. L.; Ozawa, K. *Bioorg. Med. Chem. Lett.* **2007**, *17*, 1773; (d) Miyazakia, Y.; Matsunagaa, S.; Tanga, J.; Maedaa, Y.; Nakanoa, M.; Philippea, R. J.; Shibaharaa, M.; Liub, W.; Satoa, H.; Wangb, L.; Nolteb, R. T. *Bioorg. Med. Chem. Lett.* **2005**, *15*, 2203; (e) Stieber, F.; Mazitschek, R.; Soric, N.; Giannis, A.; Waldmann, H. *Angew. Chem., Int. Ed.* **2002**, *41*, 4757.
7. Becknell, N. C.; Zulli, A. L.; Angeles, T. S.; Yang, S.; Albom, M. S.; Aimone, L. D.; Robinson, C.; Chang, H.; Hudkins, R. L. *Bioorg. Med. Chem. Lett.* **2006**, *16*, 5368.
8. (a) Gingrich, D. E.; Reddy, D. R.; Iqbal, M. A.; Singh, J.; Aimone, L. D.; Angeles, T. S.; Albom, M.; Yang, S.; Meyer, S.; Ator, M.; Robinson, C.; Ruggeri, B. A.; Dionne, C. A.; Vaught, J. L.; Mallamo, J. P.; Hudkins, R. L. *J. Med. Chem.* **2003**, *46*, 5375–5388; (b) Ruggeri, B.; Singh, J.; Gingrich, D.; Angeles, T.; Albom, M.; Chang, H.; Robinson, C.; Hunter, K.; Dobrzanski, P.; Jones-Bolin, S.; Aimone, L.; Klein-Szanto, A.; Herbert, J.-M.; Bono, F.; Schaeffer, P.; Casellas, P.; Bourie, B.; Pili, R.; Isaacs, J.; Ator, M.; Hudkins, R.; Vaught, J.; Mallamo, J.; Dionne, C. *Cancer Res.* **2003**, *63*, 5978.
9. (a) Hudkins, R. L.; Zulli, A. L.; Reddy, D. R.; Gingrich, D. E.; Tao, M.; Becknell, N. C.; Diebold, J. L.; Underiner, T. L. U.S. Patent Appl. 2005143442 A1, 2005; (b) Hudkins, R. L.; Zulli, A. L.; Reddy, D. R.; Tao, M.; Underiner, T. L. U.S. Patent Appl. 2005137245 A1, 2005.
10. Cellular activity was assessed with a VEGF-R2 autophosphorylation assay as described in Ref. 9a.
11. A TIE-2/DHI-carbazole co-crystal structure was obtained and will be reported elsewhere. The structure was refined and used for docking studies with **7e**.
12. Ruggeri, B.; Singh, J.; Gingrich, D.; Angeles, T.; Albom, M.; Chang, H.; Robinson, C.; Hunter, K.; Dobrzanski, P.; Jones-Bolin, S.; Aimone, L.; Klein-Szanto, A.; Herbert, J.-M.; Bono, F.; Schaeffer, P.; Casellas, P.; Bourie, B.; Pili, R.; Isaacs, J.; Ator, M.; Hudkins, R.; Vaught, J.; Mallamo, J.; Dionne, C. *Cancer Res.* **2003**, *63*, 5978.
13. http://www.millipore.com/drugdiscovery/svp3/profilerxl.
14. (a) Dandu, R.; Zulli, A. L.; Bacon, E.; Underiner, T.; Robinson, C.; Chang, H.; Miknyoczki, S.; Grobelny, J.; Ruggeri, B. A.; Angeles, T. S.; Aimone, L. D.; Hudkins, R. L. Presented at the 234th National Meeting of the American Chemical Society, Boston, MA, August 2007; (b) Dandu, R.; Zulli, A. L.; Bacon, E. R.; Underiner, T.; Robinson, C.; Chang, H.; Miknyoczki, S.; Grobelny, J.; Ruggeri, B. A.; Yang, S.; Albom, M. S.; Angeles, T. S.; Aimone, L. D.; Hudkins, R. L. *Bioorg. Med. Chem. Lett.* **2008**, *18*, 1916.